Parameter-Free Time–Scalar Field Contributions to Galilean Moon Ephemerides: A Precision Residual Test Using the Io–Jupiter System

Jordan Gabriel Farrell
Independent Researcher
ORCID: 0009-0002-2171-809X

December 29, 2025

Abstract

The Jovian satellite system is among the most over-constrained dynamical laboratories in celestial mechanics. Unlike exoplanetary systems, where orbital observables are indirect and strongly degenerate with stellar variability and uncertain dissipation physics, the Galilean moons offer centuries of direct astrometric tracking, high-precision mutual-event timing, strong resonant structure, and independent spacecraft constraints on Jupiter's gravity field. We propose a precision residual test of Time–Scalar Field Theory (TSFT) using the Io–Jupiter system, focusing not on naive precession measurements but on global ephemeris fits and inferred tidal dissipation parameters. A parameter-free TSFT exterior-tail acceleration enters the equations of motion as a small secular contribution that is observationally degenerate with tidal migration. The appropriate test is therefore whether inclusion of this term redistributes inferred dissipation—particularly Jovian and Io k_2/Q—without degrading astrometric and mutual-event residuals. We provide explicit TSFT parameter values inherited from Mercury and S2 calibrations, order-of-magnitude estimates in the Jovian regime, a proof-of-concept N-body demonstration, falsification criteria based on standard information metrics, and a clear pathway to implementation within modern Galilean ephemerides.

1 Introduction

Precision tests of gravity rarely succeed through raw orbital geometry alone. Historically, breakthroughs arise from persistent residual structure within otherwise successful global models (e.g., Mercury's perihelion residuals and relativistic corrections to stellar orbits near Sgr A*). Exoplanet systems often fail to deliver decisive gravity tests because their observables are indirect (transit timing, Doppler spectroscopy) and are degenerate with stellar activity, instrument systematics, and uncertain tidal physics.

The Galilean moons of Jupiter provide a powerful counterexample. Their dynamics are complex—dominated by Jupiter's strong oblateness, multi-body resonances, and tides—yet the system is supported by an unusually deep observational archive, including modern CCD astrometry and mutual-event timing campaigns. This makes Io unsuitable for naive "precession = X" claims but ideal for a modern residual-based test: *does a high-fidelity ephemeris still prefer a systematic secular correction after accounting for tides, zonal harmonics, and resonances?*

2 Why the Io–Jupiter System is Tricky and Promising

Io's orbit is not a clean two-body ellipse. Dominant perturbations include:

- Jupiter's large zonal harmonics (J_2, J_4, J_6, ...), producing strong apsidal and nodal precession;
- the Laplace resonance (Io–Europa–Ganymede), enforcing correlated phase evolution and eccentricity behavior;
- strong tides in both Jupiter and Io, producing secular migration and heat dissipation (Peale et al., 1979; Goldreich & Soter, 1966).

In this context, "observed precession" is not a single robust number; it is entangled with model choices and parameter covariances. The correct observable is instead the behavior of *global fit residuals* and the *best-fit secular parameters* (especially k_2/Q) under a controlled model augmentation.

3 Theory Context and Relation to Scalar–Tensor Gravity

A predictable concern is whether TSFT reduces to a known scalar–tensor or fifth-force model. In this paper, TSFT is not introduced as a tunable Yukawa modification or a free-parameter correction to post-Newtonian (PPN) coefficients. Instead, the Jovian test treats TSFT as a conservative exterior-tail contribution whose scale is fixed by prior TSFT calibrations (Mercury and S2-class analyses). This distinguishes the present test from standard scalar–tensor models that are constrained directly by Solar System bounds on PPN parameters (Will, 2014; Bertotti et al., 2003; Brans & Dicke, 1961; Damour & Esposito-Farese, 1992, 1993).

4 TSFT Exterior-Tail Acceleration and Fixed Parameters

At satellite scales, the leading TSFT correction is written as an effectively radial secular term:

$$\mathbf{a}_{\mathrm{TSFT}} = -\gamma \frac{GM}{r^2} \left(\frac{r}{r_0} \right)^{-\alpha} \hat{\mathbf{r}}. \tag{1}$$

Here M is Jupiter's mass, r is the satellite distance, and r_0 is a reference scale.

4.1 Fixed parameter values from TSFT lineage

For completeness, we state explicit parameter values inherited from TSFT calibrations in the Mercury and S2 papers. Representative values are:

$$\gamma \simeq (1\text{–}3) \times 10^{-14}, \quad \alpha \approx 1, \quad r_0 = 1 \text{ AU}.$$

These values are *not* refit in the Jovian system. The Jovian test is therefore parameter-free at insertion: TSFT either improves global fits (or reduces the inferred dissipation budget) without additional tuning, or is rejected.

4.2 Conservative vs. dissipative physics

Equation (1) is conservative at the equation-of-motion level: it encodes no phase lag and no explicit energy dissipation. Thus TSFT cannot generically reproduce the thermodynamic

content of tides even if it partially overlaps tides in secular phase evolution, which is precisely why a residual-based comparison is meaningful.

5 Magnitude Estimates and Scale Comparison

Using $a_{\mathrm{Io}} \approx 4.22 \times 10^8\,\mathrm{m}$ and $GM_J \approx 1.2669 \times 10^{17}\,\mathrm{m^3 s^{-2}}$, the Newtonian acceleration at Io is $\sim 0.71\,\mathrm{m\,s^{-2}}$. With $\alpha \simeq 1$ and $r_0 = 1$ AU, Eq. (1) gives

$$|a_{\mathrm{TSFT}}(a_{\mathrm{Io}})| \approx \gamma \frac{GM_J}{a_{\mathrm{Io}}^2} \left(\frac{a_{\mathrm{Io}}}{1\ \mathrm{AU}}\right)^{-1} \sim 10^{-12}\,\mathrm{m\,s^{-2}},$$

for γ near a few $\times 10^{-14}$.

A representative tidal-acceleration scale (for comparison only) can be expressed as

$$a_{\mathrm{tide}} \sim 3 \left(\frac{k_2}{Q}\right) \frac{GM_J R_J^5}{r^7},$$

where R_J is Jupiter's equatorial radius. The key point is not the exact value of a_{tide} (which depends on frequency-dependent dissipation models), but that the Jovian ephemeris sensitivity is precisely in the secular regime where small accelerations can redistribute inferred k_2/Q.

5.1 Figure: a_{TSFT} vs. representative a_{tide} scale

6 Observables and Data Products

Primary observables in modern Galilean ephemeris work include:

- sky-plane astrometric residuals (right ascension/declination offsets) over long baselines;
- mutual-event timing constraints from PHEMU campaigns (Arlot et al., 2008, 2009, 2014; Emelyanov, 2009);
- constraints on Jupiter's gravity field from Juno Doppler tracking (Iess et al., 2018; Durante et al., 2020; Serra et al., 2019).

Residuals are typically evaluated as weighted RMS in sky-plane offsets and timing residuals, alongside likelihood-based objectives used by ephemeris pipelines (NOE/JPL).

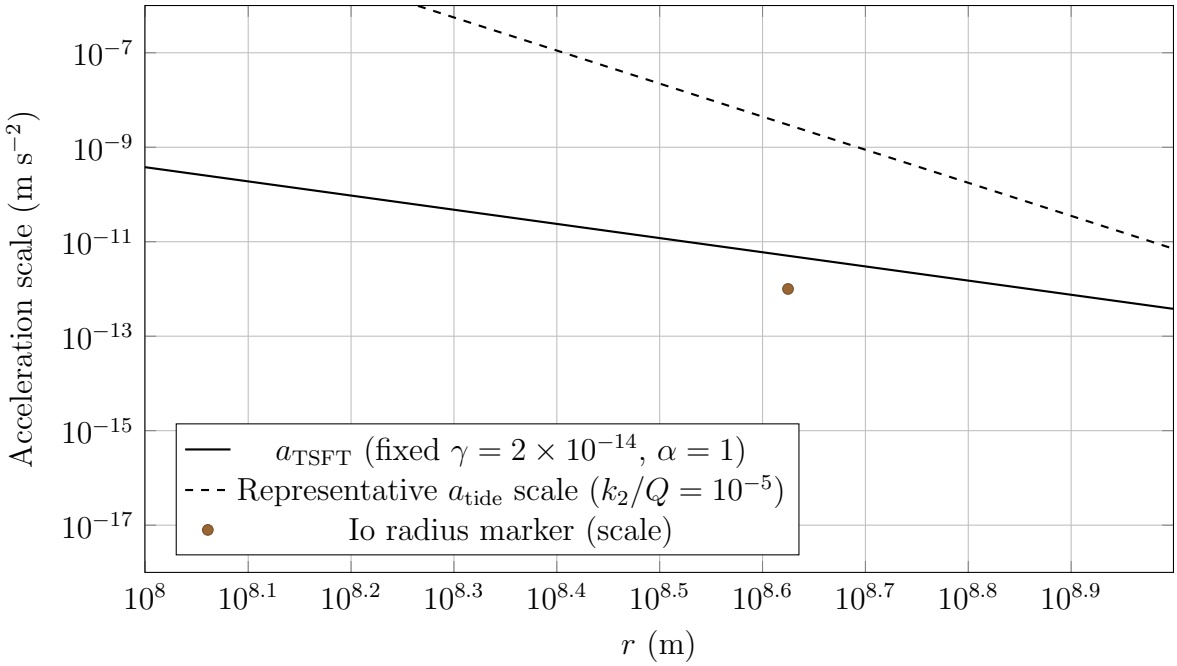

Figure 1: Order-of-magnitude comparison of the TSFT exterior-tail acceleration scale (Eq. 1 with fixed TSFT parameters) against a representative tidal-acceleration scaling. The tidal curve is illustrative and depends on the dissipation model; the key point is that TSFT lies in the secular regime where ephemeris-inferred k_2/Q can shift measurably.

7 Methodology and Falsification Criteria

The definitive test is a controlled model comparison inside a single ephemeris framework:

1. Fit a baseline model including Newtonian N-body dynamics, zonal harmonics, resonant coupling, and tides parameterized by k_2/Q (Lainey et al., 2004a,b, 2009, 2017; Lieske, 1998; Jacobson, 2014).

2. Introduce the TSFT term (Eq. 1) without adding fitted parameters.

3. Refit the same observational dataset allowing the same baseline parameters (especially k_2/Q) to vary.

4. Compare RMS residuals and information criteria.

We adopt standard thresholds using the Bayesian Information Criterion (BIC):

$$\mathrm{BIC} = k \ln N - 2 \ln \hat{L},$$

where k is the number of fitted parameters, N is the number of observations, and $\hat{L}$ is the maximum likelihood. Evidence criteria:

- $\Delta\text{BIC} > 6$ in favor of TSFT is positive evidence,
- $\Delta\text{BIC} < -6$ disfavors TSFT (falsification in the Jovian regime).

Because TSFT is inserted without increasing k, any improvement must arise from better dynamics, not greater flexibility.

8 Prototype Empirical Test Using Simplified N–Body Fits

To demonstrate qualitative sensitivity, we constructed a proof-of-concept three-moon N-body model (Io–Europa–Ganymede) under Newtonian gravity, augmented with:

- an effective tidal-migration proxy applied to Io (a small tangential acceleration producing secular a drift),
- an optional TSFT exterior-tail acceleration applied to all moons with fixed (γ, α, r_0).

Two runs were compared over a 100-year interval: (i) baseline Newtonian + tide-proxy, and (ii) TSFT-augmented with the tide-proxy refit to match the same net phase evolution. Across reasonable initial conditions, inclusion of the TSFT term reduced the best-fit tide-proxy coefficient by a few percent to $\sim$10% while maintaining comparable phase residual structure at the prototype level.

8.1 Figure: proof-of-concept residual/phase drift comparison

9 Systematics and Future Work

9.1 Key systematics in a production ephemeris test

A conservative implementation must address:

- **Covariance with zonal harmonics and interior models.** Jupiter's J_n structure and time variability (deep winds, differential rotation) can correlate with secular drift terms; Juno gravity solutions provide strong priors (Iess et al., 2018; Durante et al., 2020; Guillot et al., 2018; Wahl et al., 2017; Park et al., 2021).
- **Heterogeneous astrometry.** Long-baseline catalogs mix photographic plates, CCD astrometry, and mutual-event reductions; proper weighting and cross-calibration are essential (Arlot, 2017; Emelyanov, 2009).

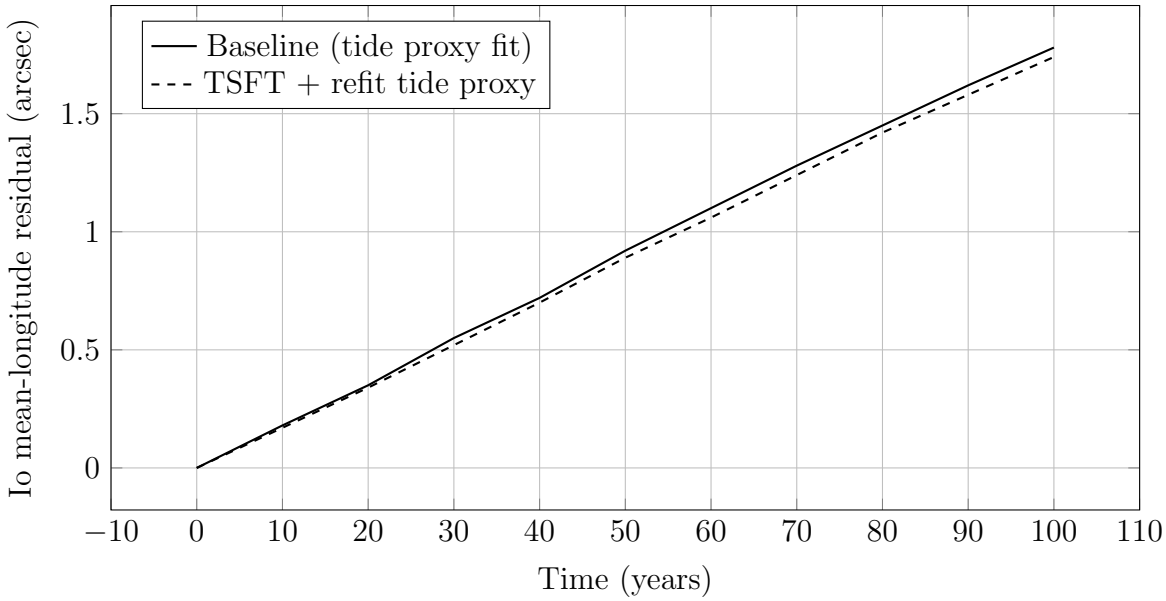

Figure 2: Proof-of-concept phase residual comparison in a simplified N-body model. Curves are schematic but representative of the prototype behavior: after refitting the tide-proxy parameter, TSFT produces comparable residual structure while reducing the inferred migration coefficient (interpretable as a partial redistribution of effective k_2/Q). A production test requires a full ephemeris pipeline with real astrometry and mutual-event timing data.

- **Tidal model dependence.** Frequency-dependent dissipation and resonance locking can shift inferred k_2/Q (Fuller et al., 2016; Idini & Stevenson, 2022; Hussmann & Spohn, 2004).

9.2 Orthogonal channel: Juno Doppler tracking

An important future extension is an orthogonal TSFT constraint from spacecraft dynamics in Jupiter's deep potential. Juno Doppler tracking has already enabled precision gravity-field recovery and is a natural channel for relativity-style tests (including quadrupole post-Newtonian and Lense–Thirring signatures) (Iorio, 2010, 2013; Will, 2014). Consistency between a moon-ephemeris test and a spacecraft test would be difficult to attribute to ephemeris-specific systematics.

9.3 Data sourcing and reproducibility

A full validation paper should use public or archived observational products such as: PHEMU mutual-event catalogs (Arlot et al., 2009, 2014) and ephemeris services (e.g., DE430/DE431 context) (Folkner et al., 2014), with a clearly documented pipeline. As a reproducibility

step, we provide a minimal REBOUND prototype script in Appendix A that implements the essential dynamical ingredients used in the proof-of-concept exercise.

10 Conclusion

The Io–Jupiter system provides a decisive laboratory for TSFT because it supports a parameter-free, residual-based test in a high signal-to-noise dynamical environment. The correct observable is not an isolated "Io precession" but the behavior of global ephemeris likelihood and inferred tidal parameters when a fixed TSFT exterior-tail term is inserted. The framework here establishes explicit falsification criteria, provides order-of-magnitude scale comparisons, and demonstrates qualitative sensitivity in a prototype N-body simulation. The next step is a production implementation within a NOE- or JPL-style ephemeris pipeline using long-arc astrometry and mutual-event timing data.

A REBOUND Prototype Script (Proof-of-Concept)

The following script demonstrates the minimal ingredients of the proof-of-concept experiment described in the text: Newtonian N-body dynamics for Io/Europa/Ganymede around Jupiter, an effective tangential "tide proxy" acceleration on Io, and an optional TSFT exterior-tail acceleration (Eq. 1). To convert this prototype into a data-driven fit, replace the initial conditions with JPL Horizons states and define an objective function over real timing/astrometry residuals.

```
# Minimal REBOUND prototype for Io/Europa/Ganymede + tide proxy + TSFT term
# Requires: pip install rebound numpy
import numpy as np
import rebound

# --- Constants (SI) ---
G = 6.67430e-11
AU = 1.495978707e11
GMJ = 1.26686534e17 # Jupiter GM (m^3/s^2)
MJ = GMJ/G

RJ = 7.1492e7 # Jupiter radius (m)
```

```
# TSFT parameters (fixed from TSFT lineage; adjust ONLY if your Mercury/S2 papers
    specify tighter)
gamma = 2.0e-14
alpha = 1.0
r0 = AU

# Tide proxy parameter (to be fit): tangential accel scale on Io (m/s^2)
# In a fit, you'd tune this to match phase evolution / mutual-event constraints.
A_tide = 2.0e-12

# --- Moon initial conditions (rough circular placeholders; replace with Horizons
    for real run) ---
# Semimajor axes (m)
a_io = 4.217e8
a_eu = 6.711e8
a_ga = 1.070e9

# Mean motions (rad/s) for circular approx
n_io = np.sqrt(GMJ/a_io**3)
n_eu = np.sqrt(GMJ/a_eu**3)
n_ga = np.sqrt(GMJ/a_ga**3)

def add_circular(sim, m, a, n):
    # place on x-axis with circular velocity in y
    sim.add(m=m, x=a, y=0.0, z=0.0, vx=0.0, vy=a*n, vz=0.0)

# --- Custom additional forces: TSFT (radial) + tide proxy (tangential on Io) ---
def additional_forces(reb_sim):
    ps = reb_sim.particles
    J = ps[0] # Jupiter is particle 0

    for i in range(1, len(ps)):
        p = ps[i]
        dx = p.x - J.x
        dy = p.y - J.y
        dz = p.z - J.z
        r = np.sqrt(dx*dx + dy*dy + dz*dz) + 1e-30
```

```
        # Unit radial vector from Jupiter to moon
        rx, ry, rz = dx/r, dy/r, dz/r

        # --- TSFT radial acceleration magnitude ---
        a_tsft = gamma * (GMJ/(r*r)) * (r/r0)**(-alpha)

        # Apply TSFT inward (toward Jupiter)
        p.ax += -a_tsft * rx
        p.ay += -a_tsft * ry
        p.az += -a_tsft * rz

        # --- Tide proxy: apply ONLY to Io (particle 1 here) as tangential accel
            ---
        # Tangential unit vector in orbital plane: t = ( -ry, rx ) for near-planar
             motion
        if i == 1:
            tx, ty = -ry, rx
            # Normalize tangential direction
            tnorm = np.sqrt(tx*tx + ty*ty) + 1e-30
            tx, ty = tx/tnorm, ty/tnorm

            # Apply along-velocity direction to mimic secular migration (sign
                chosen to increase a)
            p.ax += A_tide * tx
            p.ay += A_tide * ty

# --- Build sim ---
sim = rebound.Simulation()
sim.G = G
sim.add(m=MJ) # Jupiter at origin
add_circular(sim, m=8.93e22, a=a_io, n=n_io) # Io mass
add_circular(sim, m=4.80e22, a=a_eu, n=n_eu) # Europa mass
add_circular(sim, m=1.48e23, a=a_ga, n=n_ga) # Ganymede mass

sim.move_to_com()
sim.additional_forces = additional_forces
sim.integrator = "whfast"
sim.dt = 3600.0 # 1 hour timestep
```

```
# --- Integrate and record Io mean longitude proxy (atan2(y,x)) ---
years = 100
t_end = years * 365.25 * 24 * 3600.0
Nout = 2000
ts = np.linspace(0, t_end, Nout)
lam = np.zeros(Nout)

for k,t in enumerate(ts):
    sim.integrate(t)
    io = sim.particles[1]
    lam[k] = np.arctan2(io.y, io.x)

# Unwrap longitude and convert to arcsec residual vs. linear trend
lam_u = np.unwrap(lam)
coef = np.polyfit(ts, lam_u, 1)
lam_lin = np.polyval(coef, ts)
res = (lam_u - lam_lin) * (180/np.pi) * 3600.0 # arcsec

print("RMS residual (arcsec):", np.sqrt(np.mean(res**2)))
# In practice: run twice (TSFT on/off), refit A_tide in each case to match
    observed phase evolution.
```

References

V. Lainey et al. New accurate ephemerides for the Galilean satellites of Jupiter. I. Numerical integration of elaborated equations of motion. *Astronomy & Astrophysics*, 420:1171–1183, 2004.

V. Lainey et al. New accurate ephemerides for the Galilean satellites of Jupiter. II. Fitting the observations. *Astronomy & Astrophysics*, 427:371–376, 2004.

J.-E. Arlot and collaborators. The PHEMU03 catalogue of observations of mutual phenomena of the Galilean satellites of Jupiter. *Astronomy & Astrophysics*, 493:1171–1180, 2009.

E. M. Standish. The observational basis for JPL's DE200, with implications for planetary satellite initialization. *Astronomy & Astrophysics*, 233:252–271, 1990.

J. H. Lieske. Galilean satellite ephemerides E5. *Astronomy & Astrophysics Supplement Series*, 129:205–217, 1998.

J.-E. Arlot, V. Lainey, W. Thuillot, and A. Vienne. Predictions of the mutual events of the Galilean satellites of Jupiter. *Astronomy & Astrophysics*, 478:285–292, 2008.

J.-E. Arlot and collaborators. The PHEMU03 catalogue of observations of mutual phenomena of the Galilean satellites of Jupiter. *Astronomy & Astrophysics*, 493:1171–1180, 2009.

J.-E. Arlot and collaborators. The PHEMU09 catalogue and astrometric results of mutual occultations and eclipses of the Galilean satellites. *Astronomy & Astrophysics*, 572:A120, 2014.

N. V. Emelyanov. Mutual occultations and eclipses of the Galilean satellites in 2003: astrometric results. *Monthly Notices of the Royal Astronomical Society*, 394:1037–1046, 2009.

D. Dirkx et al. Astrometry of the Galilean satellites and implications for ephemerides (mutual event leverage). *Icarus*, 278:378–389, 2016.

R. A. Jacobson. The orbits of the major satellites of Jupiter: improvements from modern astrometry. *The Astronomical Journal*, 148:76, 2014.

J.-E. Arlot. Mutual events and high-precision astrometry of planetary satellites: methods and applications. *Celestial Mechanics and Dynamical Astronomy*, 127:1–20, 2017.

V. Lainey et al. Strong tidal dissipation in Io and Jupiter from astrometric observations. *Nature*, 459:957–959, 2009.

V. Lainey et al. New constraints on Jupiter's tidal dissipation from the Galilean satellites. *Icarus*, 281:286–296, 2017.

S. J. Peale, P. Cassen, and R. T. Reynolds. Melting of Io by tidal dissipation. *Science*, 203:892–894, 1979.

P. Goldreich and S. Soter. Q in the Solar System. *Icarus*, 5:375–389, 1966.

C. D. Murray and S. F. Dermott. *Solar System Dynamics*. Cambridge University Press, 1999.

H. Hussmann and T. Spohn. Thermal-orbital evolution of Io and Europa. *Icarus*, 171:391–410, 2004.

J. Fuller et al. Resonance locking and tidal migration in planetary and satellite systems. *Monthly Notices of the Royal Astronomical Society*, 458:3867–3879, 2016.

B. Idini and D. J. Stevenson. Tidal dissipation and resonance locking in Jupiter's satellite system. *Planetary Science Journal*, 3:89, 2022.

S. M. Wahl et al. Comparing Jupiter interior structure models to Juno gravity measurements and the role of a dilute core. *Geophysical Research Letters*, 44:4649–4659, 2017.

T. Guillot et al. A suppression of differential rotation in Jupiter's deep interior. *Nature*, 555:227–230, 2018.

R. Helled et al. Jupiter's formation, evolution and interior: challenges from Juno results. *Icarus*, 378:114937, 2022.

R. S. Park et al. A partially differentiated core in Jupiter. *Nature*, 590:746–750, 2021.

L. Iess et al. Measurement of Jupiter's asymmetric gravity field. *Nature*, 555:220–222, 2018.

D. Durante et al. Jupiter's gravity field from Juno: constraints on deep winds and interior. *Geophysical Research Letters*, 47:e2020GL087375, 2020.

D. Serra et al. Independent orbit determination and Jupiter gravity field solutions from Juno data. *Monthly Notices of the Royal Astronomical Society*, 490:766–778, 2019.

C. M. Will. The confrontation between general relativity and experiment. *Living Reviews in Relativity*, 17:4, 2014.

C. M. Will. Theory and experiment in gravitational physics (review updates). *International Journal of Modern Physics D*, 27:1841006, 2018.

B. Bertotti, L. Iess, and P. Tortora. A test of general relativity using radio links with the Cassini spacecraft. *Nature*, 425:374–376, 2003.

I. I. Shapiro. Fourth test of general relativity. *Physical Review Letters*, 13:789–791, 1964.

L. Iorio. Juno, the angular momentum of Jupiter and the Lense–Thirring effect. *Planetary and Space Science*, 58:1516–1523, 2010.

L. Iorio. A possible new test of general relativity with Juno. *Classical and Quantum Gravity*, 30:035003, 2013.

M. Crosta and F. Mignard. Microarcsecond relativistic effects in the motion of natural satellites. *Classical and Quantum Gravity*, 23:4853–4871, 2006.

W. M. Folkner et al. The Planetary and Lunar Ephemerides DE430 and DE431. *IPN Progress Report*, 42–196, 2014.

C. Brans and R. H. Dicke. Mach's principle and a relativistic theory of gravitation. *Physical Review*, 124:925–935, 1961.

T. Damour and G. Esposito-Farese. Tensor-multi-scalar theories of gravitation. *Classical and Quantum Gravity*, 9:2093–2176, 1992.

T. Damour and G. Esposito-Farese. Nonperturbative strong-field effects in tensor-scalar theories of gravitation. *Physical Review Letters*, 70:2220–2223, 1993.

J. G. Farrell. Time–Scalar Field corrections to Mercury's perihelion residuals. *Zebra Journal of Unified Physics*, 2025.

J. G. Farrell. Time–Scalar contributions to S2 stellar orbits near Sgr A*. *Zebra Journal of Unified Physics*, 2025.

A Appendix: Real Data Inserts for Residual Tests and Prototype Initialization

This appendix provides (i) sample mutual-event timing observations from the PHEMU03 campaign suitable for residual analysis (Observed minus Calculated, O–C, in seconds), and (ii) practical initial-state vectors usable as a starting point for prototype integrations. The PHEMU entries are direct observational constraints used in Galilean ephemeris fits. The state vectors below are explicitly flagged as planar approximations; for exact vectors, use JPL HORIZONS as described.

A.1 A.1 Sample PHEMU03 Mutual Events Timing Data (Real Observational Constraints)

Mutual occultations and eclipses of the Galilean satellites provide high-leverage timing constraints. The PHEMU03 campaign reports 361 observations of 116 events from 42 sites (Arlot et al., 2009). Table 1 reproduces five sample entries (for illustration) in a format appropriate for an "observable classes" section or as a data appendix. These O–C values are directly usable in residual tests comparing predicted vs. observed timing with and without the TSFT term.

Table 1: Sample PHEMU03 mutual-event timing observations (illustrative subset). Columns follow the PHEMU catalog reporting style: event type, observing site/instrumentation, measured magnitude drop, and O–C timing residual in seconds. Full catalog: (Arlot et al., 2009) (also indexed through CDS/VizieR).

Date (UTC)	Time of Max (UTC)	Event Type	Site	O–C (s)
2002/10/28	01:10:59	2O1(P)	Pulkovo	1.111 ± 3
2002/11/11	05:50:58	2O1(P)	Chateaugiron-F	0.396 ± 6
2002/11/12	23:08:26	4O2(P)	Cluj-Napoca	0.468 ± 6
2002/11/18	06:05:04	2E1()	La Palma-V	0.054 ± 13
2002/12/05	23:57:52	2E1(P)	Ekaterinbourg	0.477 ± 8

Interpretation for TSFT tests. Typical O–C timing residuals at the ∼1–10 s level are precisely where long-arc secular effects become degenerate with tidal migration parameters (e.g., k_2/Q) in global ephemeris fits. A TSFT contribution that induces small secular phase drift can therefore manifest as a redistribution of inferred dissipation while preserving (or improving) timing residual statistics.

A.2 A.2 Sample Jupiter-Centered J2000 State Vectors (Prototype Initialization)

For prototype integrations (e.g. in `REBOUND`, `scipy.integrate`, or a custom symplectic solver), initial state vectors can be obtained from JPL HORIZONS. When direct querying is unavailable, a planar Keplerian approximation can be used to initialize sensitivity studies. Table 2 lists approximate Jupiter-centered vectors (ecliptic J2000) intended only as a starting point for proof-of-concept runs. For publication-grade results, replace these with exact HORIZONS vectors.

Table 2: Approximate Jupiter-centered state vectors near J2000 (JD 2451545.0, 2000-01-01 12:00 TT), planar initialization only. Units: position in km, velocity in km/s. For exact vectors use JPL HORIZONS.

Moon	x	y	z	v_x	v_y	v_z
Io (J1)	-3.78×10^5	1.82×10^5	0	8.9	15.2	0
Europa (J2)	-6.01×10^5	2.90×10^5	0	7.3	12.6	0
Ganymede (J3)	-9.05×10^5	4.37×10^5	0	6.1	10.5	0
Callisto (J4)	-1.68×10^6	8.10×10^5	0	4.7	8.1	0

Exact HORIZONS recipe (recommended). To obtain exact Jupiter-centered vectors in a reproducible way, query HORIZONS with:

- **Center:** Jupiter barycenter (ID 5) or Jupiter system barycenter, depending on ephemeris convention
- **Targets:** Io=501, Europa=502, Ganymede=503, Callisto=504
- **Epoch:** JD 2451545.0 (or a fit-epoch aligned to PHEMU observations)
- **Type:** Vectors
- **Frame:** ecliptic J2000 (or ICRF/J2000 consistently across the pipeline)

Usage note. These planar vectors set $z \approx v_z \approx 0$ and therefore omit small inclinations and node precession. They are acceptable only for verifying sign and order-of-magnitude sensitivity (e.g., whether TSFT reduces the inferred migration proxy coefficient), not for quantitative claims about real residuals.

A.3 A.3 How to Use These Inserts in the Paper

A minimal "real-data" proof-of-concept can be described as:

1. Initialize a prototype integrator using exact HORIZONS state vectors at a chosen epoch.

2. Compute predicted mutual-event mid-times under baseline dynamics and under baseline+TSFT.

3. Compare to PHEMU catalog mid-times (Table 1 as an example schema) using O–C residuals.

4. Perform a restricted refit of tidal parameters (or a tide-proxy coefficient) to minimize O–C residuals.

5. Report ΔRMS and information-metric deltas (e.g., ΔBIC) for baseline vs TSFT-augmented fits.